

Evidence of Radical Intermediate Generated in the Electrochemical Oxidation of Iodide

Ashantha Fernando^{1a}, Suman Parajuli^{1b}, Krishna K. Barakoti¹, Wujian Miao², and Mario A. Alpuche-Aviles^{1*}

¹Department of Chemistry, University of Nevada, Reno, Nevada 89557, USA

²Department of Chemistry and Biochemistry, The University of Southern Mississippi, Hattiesburg, Mississippi, 39406, USA.

^aCurrent address: Department of Chemistry, Susquehanna University, Selinsgrove, Pennsylvania, USA.

^bCurrent address: Arizona Western College, Yuma, Arizona, USA.

***Corresponding author:** Mario A. Alpuche-Aviles, e-mail: malpuche@unr.edu

Received March 30th, 2018; Accepted April 12th, 2018.

DOI for the main article: <http://dx.doi.org/10.29356/jmcs.v63i3.529>

Supplementary Information

Table of Contents

I.	Scan Rate Dependence of Oxidation Currentes af FTO.....	3
II.	Additional CVs of Iodine species on FTO.....	3
III.	Cyclic voltammetry of TMPO and DMPO.....	4
IV.	Oxidation of Bromide.....	4
V.	Photochemically Generated Iodine Atoms.....	5
VI.	Spectroelectrochemistry.....	6
VII.	Long Term Electrolysis.....	7
VIII.	Gas Chromatography – Mass Spectrometry (GCMS) Studies of Long Term Electrolyzed Samples.....	8
	Reference.....	11

I. Scan Rate Dependence of Oxidation Currents at FTO

The scan rate dependence of first and second oxidation waves of Γ^- at FTO was studied to investigate whether these oxidation processes are limited by diffusion or surface confined. Fig. S1. shows that the peak anodic currents (i_{pa}) for both the waves in Fig. 1 in the manuscript present a linear relationship with the square root of the scan rate, the two oxidation steps of Γ^- at FTO are limited by diffusion.

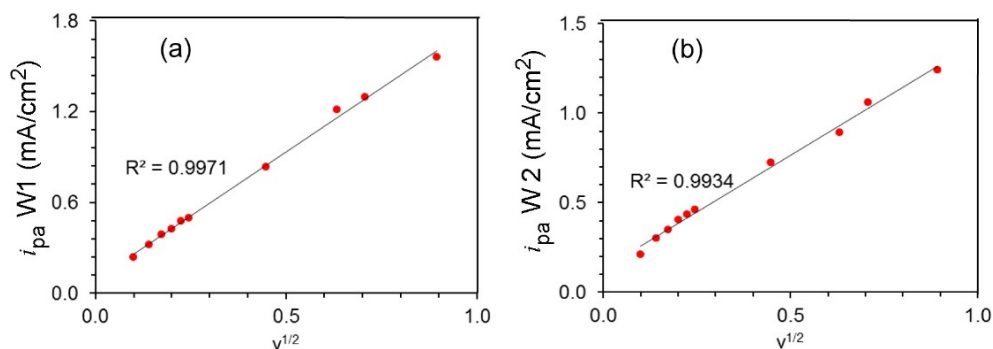


Fig. S1. Scan rate dependence of the peaks in for the first (a) and the second (b) oxidation waves of a 1 mM TBAI at different scan rates. All other conditions as in Fig. 1.

II. Additional CVs of Iodine species on FTO.

Fig. S2 shows the control CVs performed with different solution of iodide precursors. Fig. S2a shows the same data as Fig. 1 in the manuscript, but note the different axis scales. Fig S2b shows that the oxidation Γ^-/I_3^- is kinetically irreversible because it is shifted to considerably negative potentials. When the potential scan in the anodic direction is large, the reduction of I_2 appears as the peak marked as A1.

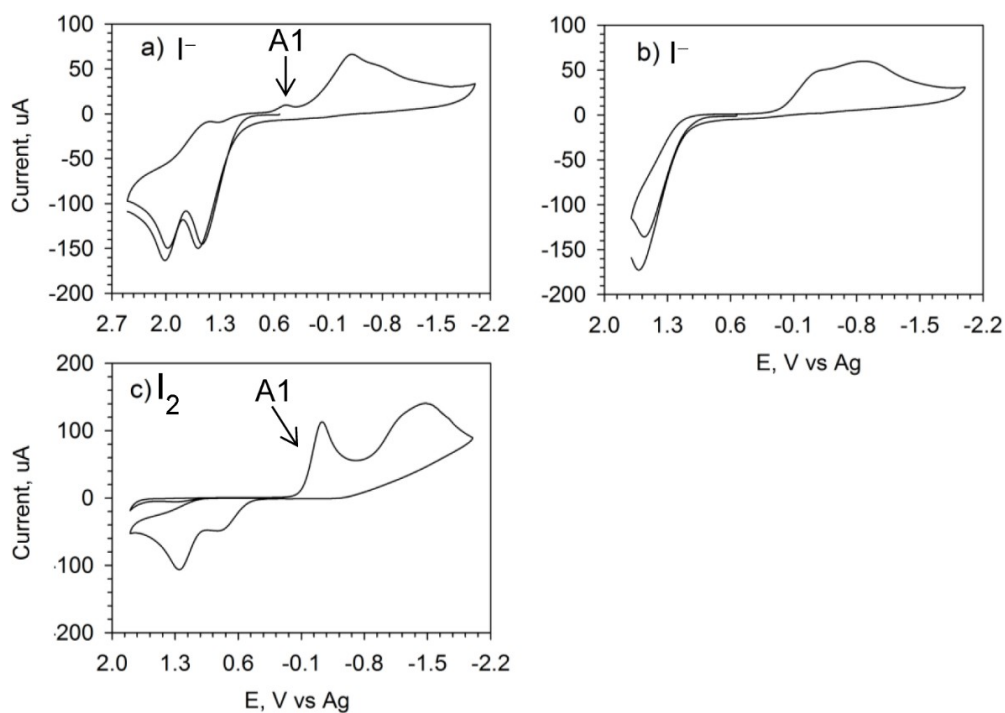


Fig. S2. CVs of iodine species (a) 1 mM I^- , (b) 1 mM I^- with a different scan window. Note the shift of the I_3^- reduction peak. and c) 1 mM I_2

III. Cyclic voltammetry of TMPO and DMPO.

Fig. S3 shows the CVs for the radical traps used in this study. Fig. S3a shows the CV of DMPO on an FTO electrode; at the potentials of interest, ca. 1.9 V the DMPO starts to oxidize on FTO electrodes. Thus, the use of TMPO was preferred. Note that while their oxidation potentials are similar, on FTO the oxidation of TMPO is shifted to potentials significantly more positive potentials than the potentials used in the electrolysis experiments, ca. 1.9 V. Fig S3(b) is the CV of TMPO on Pt electrode; although on Pt the oxidation starts at potentials less positive of 2 V, on FTO the onset of the oxidation is shifted to more positive potentials as shown on (c) and (d).

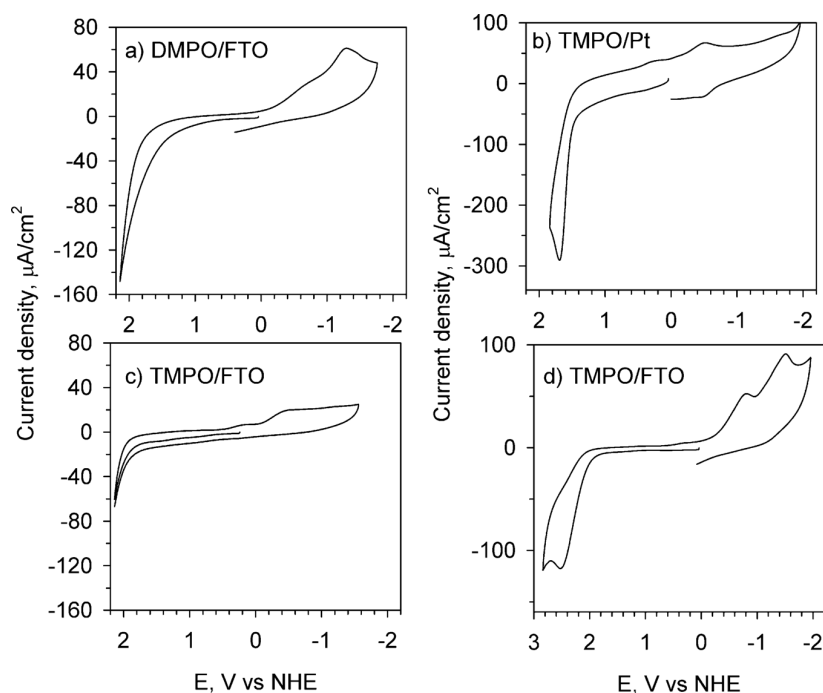


Fig. S3. CVs the traps used in these studies. All concentrations 1 mM . (a) Shows the CV of DMPO on FTO. (b) is the CV of TMPO on Pt electrode; although on Pt the oxidation starts at potentials less positive of 2 V, on FTO the onset of the oxidation is shifted to more positive potentials as shown on (c) and (d)

IV. Oxidation of Bromide

The first and the second oxidation of bromide occurs at $E_p = 2.25$ V and $E_p = 2.92$ V vs NHE respectively, as seen in Fig. S4.

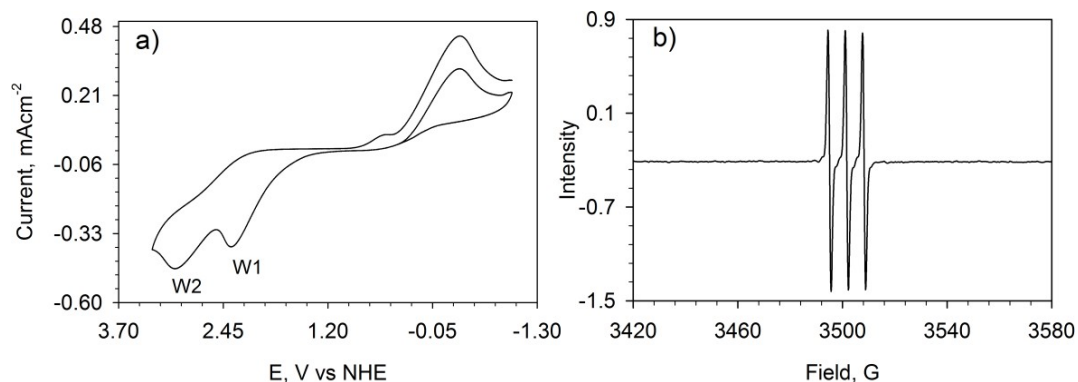


Fig. S4. a) CV of 1 mM TBABr in CH_3CN at FTO electrode. 0.1 M TBAP was used as the supporting electrolyte. b) EPR signal obtained with 30 mM of TMPO. The solution was electrolyzed for 30 min at $E_{p,W2} = 2.9$ V vs NHE prior adding TMPO.

Because the second oxidation of bromide appears at a more positive potentials than the oxidation of TMPO (Fig. S3), in this experiment TMPO was added after applying the potential step of 2.9 V vs NHE for 30 minutes. For this we did not observed a significant color change during the time period of electrolysis.

V. Photochemically Generated Iodine Atoms.

Experimental Details. The experimental procedure for the photogeneration of I^\bullet in brief, a solution of 1 mM iodine in CH_3CN , containing in fluorescent cuvette (1 cm path length, Starna Cells, Inc), was purged with Ar for 20 min and sealed with a cap. The sample was illuminated with 150 W Xe lamp for 30 minutes. Subsequently, a 30 mM TMPO solution was added into the sample. The illumination was stopped immediately after the addition of TMPO to prevent any photooxidation of TMPO.

The reactivity of photogenerated I^\bullet with CH_3CN was studied. In this case, a set of experiments were performed to examine the product of the reaction. If the photogenerated I^\bullet react with TMPO to form Γ as depicted in Fig. 4, we would expect a similar reactivity with CH_3CN as shown in Fig. S6. However, we also expect I_3^- formation instead because the solvent contains I_2 . In order to accumulate a detectable amount of I_3^- , a sample of 10 mM iodine in CH_3CN sealed under Ar was constantly illuminated for 19 hours. Subsequently, an UV Visible spectrum was obtained shown in Fig. S5. The UV Visible spectrum of the solution after 19 h of illumination shows two specific peaks at 291 nm and 361 nm which do not appear at the beginning of the experiment. These peaks correspond to I_3^- in CH_3CN [1]. Another peak at 250 nm can be seen due to byproducts of the photochemical reaction.

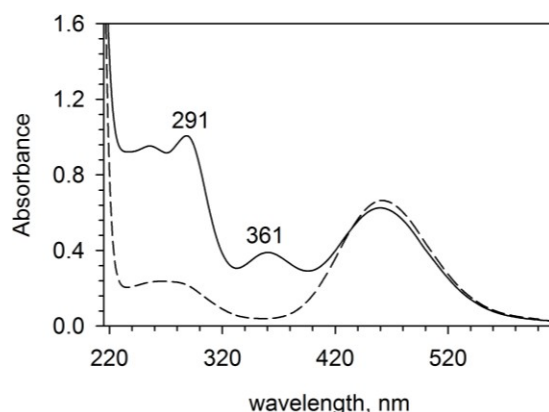


Fig. S5. 10 mM iodine in CH_3CN under Ar. (---) before illumination and (□□) after 19 h of constant illumination. A fluorescent cuvette of 1 cm path length was used as the sample container and the illumination was done using 150 W Xe lamp.

Fig. S6 shows the mechanism proposed to explain the formation of I_3^- after the reaction of photogenerated I^\bullet with CH_3CN .

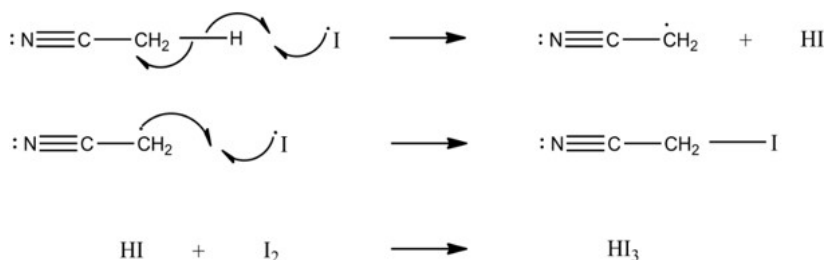


Fig. S6. Proposed mechanism for I_3^- formation during the illumination of I_2 in CH_3CN .

UV Visible spectra were obtained for the above illuminated sample with time: the absorbance for peaks at 291 nm and 361 nm were recorded with time after illumination for 19 h and shown in Fig. S7. Interestingly, the peaks for I_3^- grew continuously in the dark. This behavior indicates a mechanism that propagates after initiation, consistent with the proposed mechanism in Fig. S6.

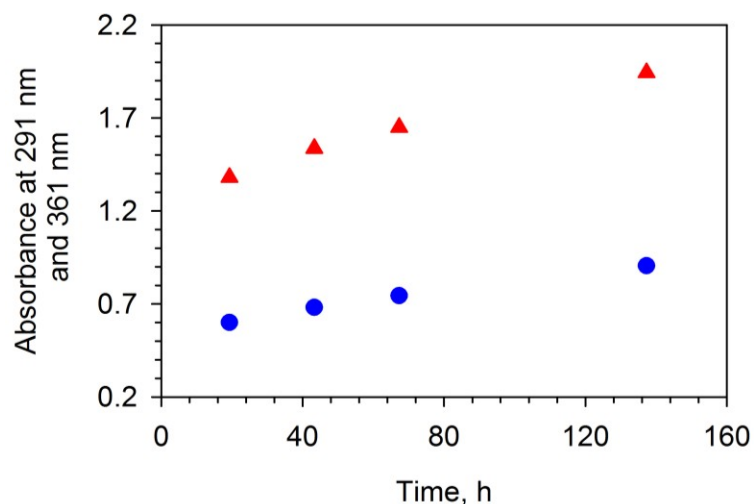


Fig. S7. The absorbance of I_3^- vs. time after 19 h of illumination of a sample containing 10 mM iodine in CH_3CN under Ar. (Δ) absorbance at 361 nm and (●) absorbance at 291 nm.

VI. Spectroelectrochemistry

A spectroscopic method was implemented to study the formation of iodine species during the electrochemical oxidation of I^- at FTO. The potential step of 1.9 V vs NHE was applied to the sample cell and UV visible spectra were recorded simultaneously. The formation of I_3^- (gives two characteristic peaks at 291 nm and 361 nm), [1] was observed during the electrolysis and it is shown in Fig. S8.

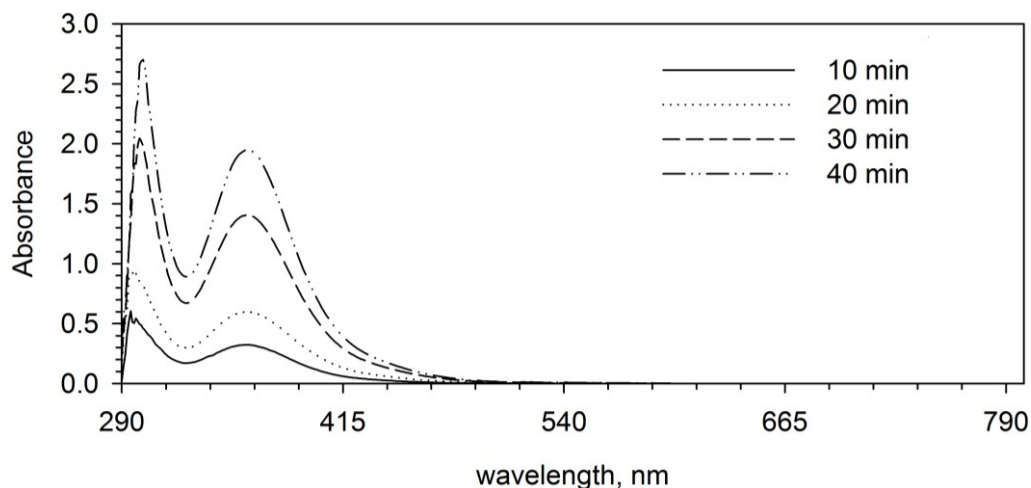


Fig. S8. The UV Visible spectra of the oxidized species of I^- recorded with time. Electrolyte is 1mM TBAI, 0.1 M TBAP in CH_3CN . The spectra were recorded while applying the potential step of 1.9 V vs NHE.

Note that the cutoff for our measurement was ca. 290 nm because FTO coated glass substrate absorbs light below this wavelength. Attempts were made to observe for any indication of the existence of $I^{\cdot -}$ in our system ($I^{\cdot -}$ shows a characteristic peak around 710 nm) [1]. However, we have not observed any significant changes in the spectrum in the range of 500 nm to 800 nm, consistent with our expectation that the concentration of $I^{\cdot -}$ should be negligible near the surface of the FTO electrode.

VII. Long Term Electrolysis.

Long term electrolysis was performed for $I^{\cdot -}$ in CH_3CN at FTO to accumulate an adequate amount of product of the radical reaction. The $I^{\cdot -}$ forms during the electrolysis of I^- , there is a high possibility for it to react either with the solvent molecules or with TBA^+ to produce stable products. Therefore, a sample of 1 mM TBAI, 0.1 M TBAP in CH_3CN was electrolyzed at FTO electrode for 17 hours continuously and UV Visible spectrum was obtained. The potential applied was 1.9 V vs NHE.

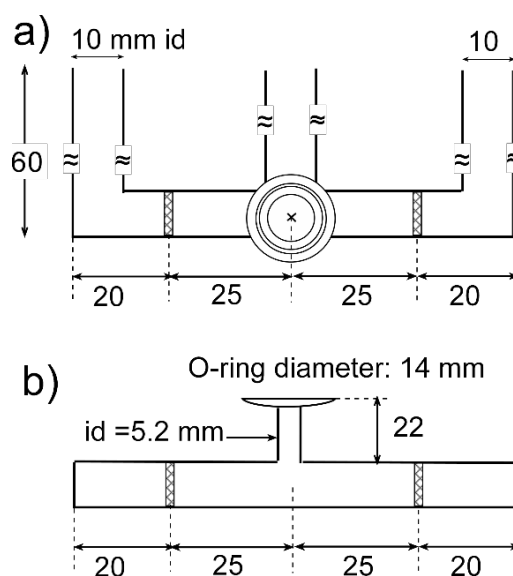


Fig. S9. Diagram of the long-term electrolysis cell (not drawn to scale), all dimensions in millimeters, including the inner diameter (id) of the glass tubing. a) shows a later view and (b) a view from the bottom of the cell.

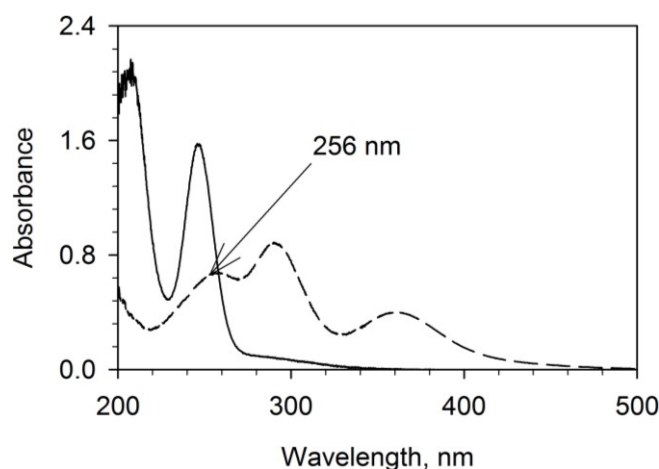


Fig. S10. UV Visible spectrum obtained for 1 mM TBAI, 0.1 M TBAP in CH_3CN after the electrolysis of 17 h at FTO working electrode. The $E_{\text{app}} = 1.9 \text{ V}$ vs NHE. The solid line and the dashed line represent the data obtained before and after the electrolysis respectively. The baseline was corrected for 0.1 M TBAP in CH_3CN before collecting data.

The UV Visible spectrum of the electrolyte before the electrolysis (solid line) shows two peaks at 208 nm and 246 nm which is characteristic for I^- [1]. The spectrum obtained after the 17 h of electrolysis (dashed line) shows four distinguished peaks where peaks at 291 nm and 361 nm represent I_3^- and the peak appearing below 225 nm represents I_2 . The extra peak appearing at 256 nm should be due to the result of I^\cdot reacting either with the solvent or with TBA^+ . If I^- only gets oxidized to I_3^- and subsequently to I_2 , after 17 h of electrolysis the only probable species in the solution should be only I^- , I_3^- and I_2 . Having an extra peak after long run electrolysis at 256 nm indicates an ongoing additional reaction consistent with the formation of I^\cdot during the second oxidation of iodide at FTO electrode.

VIII. Gas Chromatography – Mass Spectrometry (GCMS) Studies of Long Term Electrolyzed Samples

We used GC-MS to characterize the final products of the radical reaction. The electrochemical samples for GCMS were prepared by electrolyzing 0.1 M tetrabutylammonium iodide (TBAI) in CH_3CN at FTO working electrode for 20 h. The $E_{\text{app}} = 3.5 \text{ V}$ vs Ag. No additional TBAP was added. The electrolyzed solution was used directly without further purification.

Parameters. GC-MS analyses were performed on Agilent Technologies 7890 A GC systems coupled with a 5975 C inert Mass Selective Detector (MSD) with triple-axis detector mass spectrometer. The column was a HP-5MS fused-silica capillary column packed with 5% Phenyl Methyl Silox ($30\text{m} \times 250\mu\text{m} \times 0.25\mu\text{m}$) and carrier gas used was helium running at a constant pressure of 7.0699 psi. The system had auto injector and 1 microliter volumes were injected using a split mode (100:1) at an injector temperature of 250°C . The Oven temperature was ramped from 40°C to 250°C at a rate of $5^\circ\text{C}/\text{min}$. Total run time for the each sample analysis was 42 minutes. Ion source and quadrupole temperatures were set to 230°C and 150°C respectively. During analysis, Mass Spectrometry mode was used scanning from 5 to 550 atomic mass unit (amu).

Several control solutions were prepared and analyzed using GCMS and compared them with the data obtained for electrolyzed sample of I^- at FTO. The control samples that have been analyzed are, 0.1M TBAI in acetonitrile, mixture of 0.1M TBAI and 0.1M I_2 in acetonitrile, 0.1 M I_2 in acetonitrile and acetonitrile. A number of extra peaks were noticed in the GC-MS at retention times; 7.654 min, 8.665 min, 10.159 min, 19.425 min, 21.844 min, 22.129 min, 22.446 min and 28.623 min for the electrolyzed sample which does not appear in any of the controls described. We have assigned molecules representing most of the extra peaks which appear in the total ion chromatogram (Fig. S11).

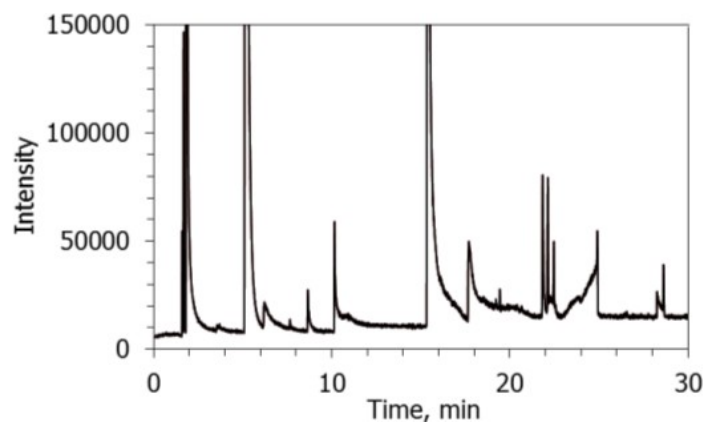


Fig. S11. Total ion chromatogram of the electrolyzed sample of 0.1 M iodide in CH₃CN. E_{app} = 2.8 V vs Ag, electrolyzed for 17 h.

The spectra obtained for the for retention times in Table 1 of the paper follow:

retention time 7.654 min

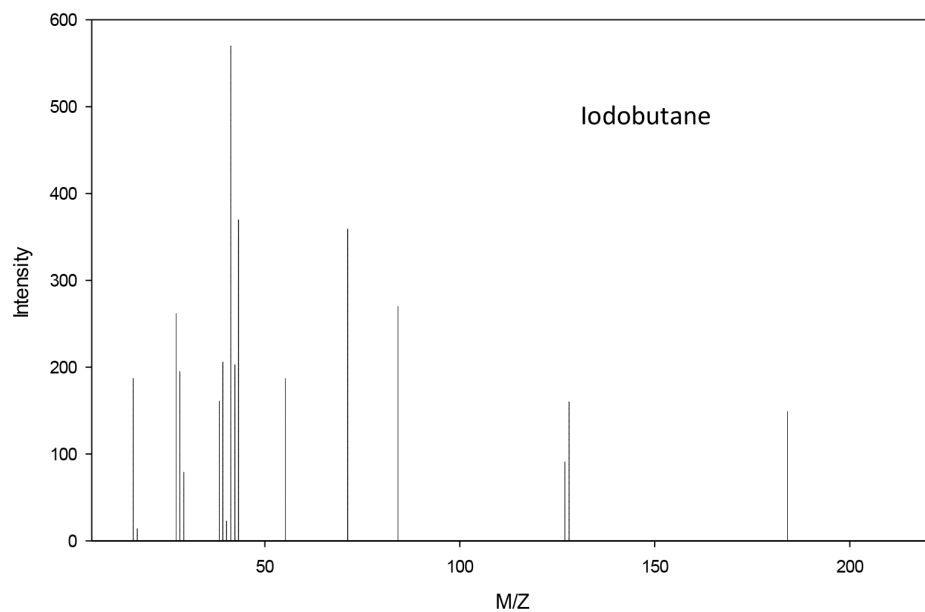


Fig. S12. Spectra obtained at 7.654 min retention time.

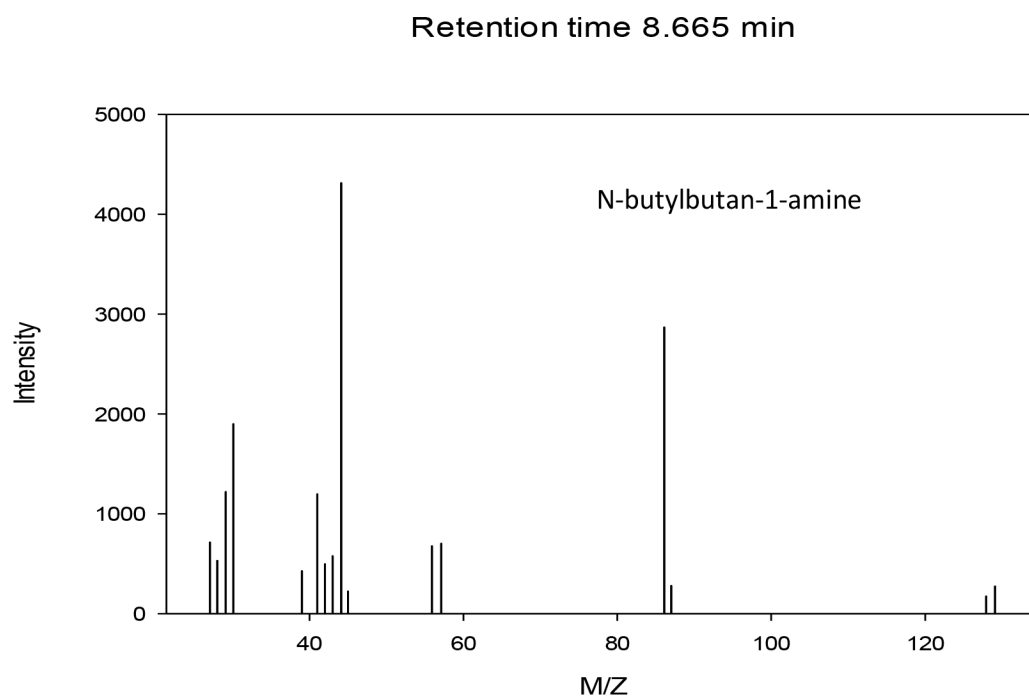


Fig. S13. Spectra obtained at 8.665 min retention time.

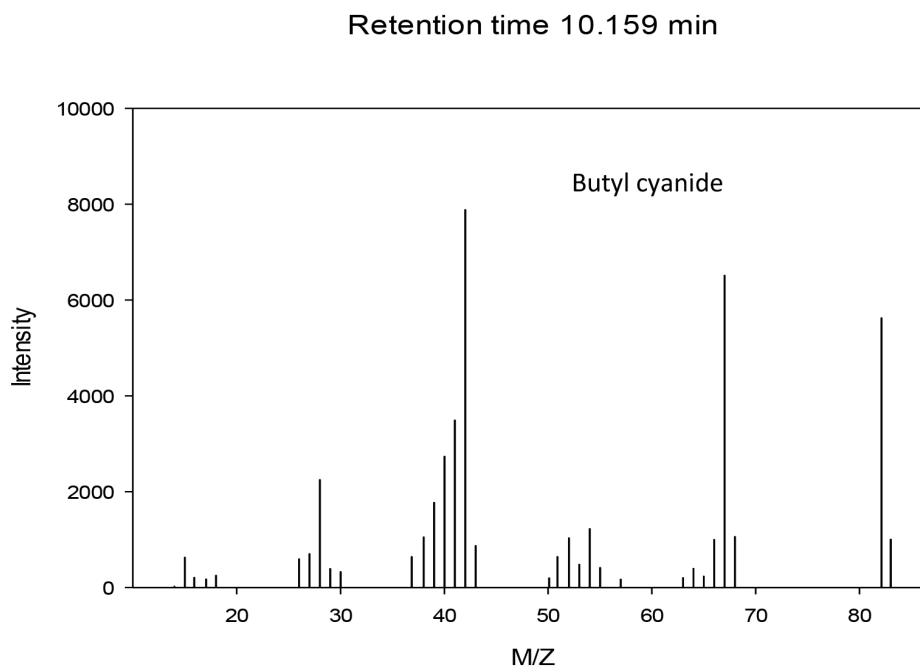


Fig. S14. Spectra obtained at 10.159 min retention time.

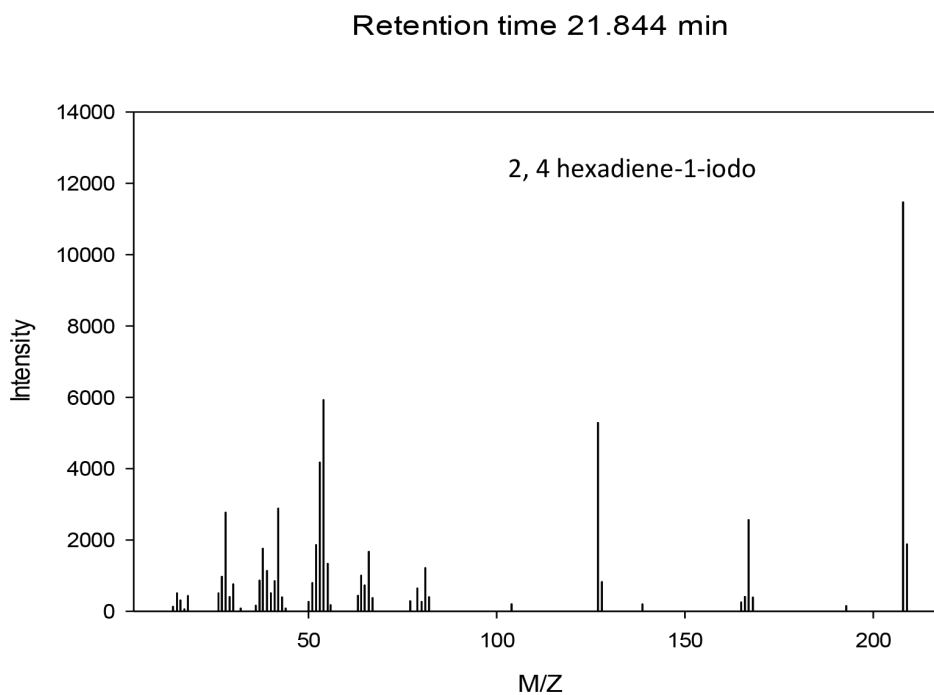


Fig. S15. Spectra obtained at 21.844 min retention time.

Reference

1. Gardner, J. M.; Abrahamsson, M.; Farnum, B. H.; Meyer, G. J. *J. Am. Chem. Soc.* **2009**, 131, 1620.